Study of the elaboration of high entropy material from powder by laser additive manufacturing

G. Huser, I. Demirci, P. Aubry, I. Guillot, L. Perrière, E. Rigal, H. Maskrot

Available online at www.sciencedirect.com

ScienceDirect

Procedia CIRP 00 (2020) 000–000

www.elsevier.com/locate/procedia

11th CIRP Conference on Photonic Technologies [LANE 2020] on September 7-10, 2020

Study of the elaboration of high entropy material from powder by laser additive manufacturing

G. Huser[a], I. Demirci[b], P. Aubry[a*], I. Guillot[c], L. Perrière[c], E. Rigal[d], H. Maskrot[a]

[a] Den – Service d'Etudes Analytiques et de Réactivité des Surfaces (SEARS), CEA, Université Paris-Saclay, F-91191, Gif sur Yvette, France, France
[b] Arts et Metiers Institute of Technology, MSMP, HESAM Université, Châlons en champagne 51006, France
[c] Univ. Paris Est Creteil, ICMPE (UMR 7182), CNRS, F-94320 Thiais, France
[d] CEA, LITEN, F-38054 Grenoble Cedex 9, France

* Corresponding author. Tel.: +33169088191 ; *E-mail address:* pascal.aubry@cea.fr

Abstract

If Stellite® 6 is a cobalt base alloy with a hard coating well known for its good wear resistance, its use is not desirable for nuclear installations due to the activation of cobalt under neutron flux which makes maintenances more delicate as, later, decommissioning. If several studies have led to propose certain hard coatings without cobalt, for the moment, none equals the wear properties of Stellite® 6.

The present research aims to explore the recent research area on high entropy alloys or concentrated composition alloys (HEA/CCA) as a new path for the development of innovative hard coatings. The study is based on the use of thermodynamics simulations with CALPHAD in order to predict the compositions of a large number of alloys, after an initial selection of the acceptable elements (NiFeCrMoTi in this study). Then, Laser Metal Deposition (LMD) is used for manufacture walls of graded compositions for a rapid screening of compositions and coatings for later wear tests. The metallurgical analyses of the elaborated samples allow selecting the most promising ones on which wear pin-on-disk tests are finally conducted. The wear tests have evidenced promising behavior for the selected HEA/CCAs.

Peer review statement: Peer-review under responsibility of the Bayerisches Laserzentrum GmbH
Keywords: Laser Metal Deposition, High Entropy Alloy, Concentreated Composition Alloy, Combinatorial Metallurgy, Hardfacing Material, CALPHAD

1. Introduction

1.1. Context of the study

The CEA is leading researches on existing nuclear reactor and innovative nuclear systems called Generation III and Generation IV reactors. They require major technological breakthroughs compared with the previous generation of reactors, particularly on materials and manufacturing processes.

Besides the structural materials, contact areas between moving components require specific wear resistant coatings with a very long timelife.

Stellite®, a cobalt based alloy is the well-known and widely used hardfacing wear resistance material from Deloro Company. Unfortunately, one major drawback of this type of alloy for nuclear applications is the activation of cobalt under neutron flux in a reaction that generate radioactive ^{60}Co. With a period of 5.7 years, the activity of ^{60}Co is maximum during operation of the reactor. Thus, it is desirable to avoid these alloys for severe neutron flow and different studies tried to find substitute material without cobalt or in very small quantities.

The requirements are very demanding: tribo-corrosion under sodium, operating temperature from 180 to 500°C, risk of thermal shock and thermal cycling, and life spam of over 60 years without binding or degradation. As a consequence, thick

Peer review statement: Peer-review under responsibility of the Bayerisches Laserzentrum GmbH

coatings (2-3mm) with little porosity, no crack and metallurgical bond between the coating and the base material are required. This implies to use a high energy fusion process that can be automatized as Plasma Transferred Arc Welding (PTAW) or Laser Metal Deposition (LMD).

If the cobalt base alloy Stellite remains the reference, other alloys have been investigated as cobalt-free alternatives. Base substrates are majorly stainless steel as 304L, 316L or 316L(N).

A large number of Co-free hardfacing materials have been proposed in the literature. Among them, we can consider two main types of materials: the iron and nickel based alloys. If iron base alloys cannot be definitely excluded, the bibliography [1, 2, 3] demonstrates a poor behavior of the iron-based hardfacing coatings at high temperature regardless of the deposition process.

On the opposite, authors have evidenced the interest of using hardfacing nickel based alloys [4,5]. For this reason, two promising nickel base alloys have been studied : NiFeCrSiBC alloys as Colmonoy®, from Wall Colmonoy Company, presented in previous publications [6-9] or NiFeCrMoSi alloys, as Tribaloy® T700, developed by Deloro Company. These materials have been tested but, up to now, none of them have provided equivalent behavior to Stellite® [10,11,12].

1.2. Interest for HEA/CCAs

Considering the composition of the alloys that have been previouslty evaluated (particularly the Tribaloy® T700), one idea to extend the research base of innovative substitute can be to consider a new family of alloys and fully new methodology for their formulation by exploring the capabilities of finding cobalt-free high entropy alloys (HEAs) or complex concentrated alloys (CCAs).

HEA is a new type of alloy without a single main constituent. Cantor [14] and Yeh [15] firstly discovered them, and explored the theory of HEAs. They are thought to be promising material in several domains. If HEAs are single solid solutions or euticties structures of multiple elements in high concentration (≥ 5at%), a dual phased or multi phased HEA is more properly named Complex Composition Alloy (CCA). Particularly, CCAs can exhibit good tribological behaviors, as precipitation of hard phases can improve hardness and wear resistance [16,17]. Consequently, cobalt-free CCAs could be interesting candidates to stellite® substitutes. Very few studies on cobalt-free HEA/CCA coatings for tribological behavior were published, and even less on stainless steel substrates [18].

For this study, Laser Metal Deposition (LMD), a laser additive manufacturing process, is the chosen process to deposit thick CCAs coatings because it is a known to be particularly adapted to deposit thick (several mm) of Stellite® coatings [1,2,4,6]. It is also a powerful process to develop new alloys as HEA/CCAs since it is possible to make in-situ alloys by co-projecting different elemental powders and mixing them inside the melt pool [19, 20, 21, 22]. It also allows massive fabrication of samples by making composition gradient and studying several composition in one sample.

CALPHAD (CALculation of PHAse Diagram) is a calculation tool of thermodynamic properties of multi_elements material as metallic alloys. It is based on thermodynamics databases of single elements and on the fact that a phase diagram is a manifestation of the equilibrium thermodynamic properties of a system, which are the sum of the properties of the individual phases [23].

CALPHAD has been used on numerous HEA/CCAs [24, 25] with accurate predictions of the microstructure. Addition of Mo and Ti to the three “base elements” NiFeCr promotes the formation of hard phases such as sigma and C14 Laves phase.

CALPHAD allows not only equilibrium but also out-of-equilibrium calculation models, as the Gulliver-Scheil approximation. As high solidification speed and cooling rates result from the LMD process, this will be considered in the study.

At the beginning of the research, it is proposed that CALPHAD calculations could be a tool for an initial selection of composition, avoiding extended experimental investigations. Consequently, a methodology, presented in the next section, is proposed and will be the common thread of this article.

1.3. Methodology

A proposed methodology, sketched in Fig. 1, is applied to our HEA/CCAs developments:

- A first set of alloys is selected form the bibliography analyses and material data.
- Composition of alloys after solidification are forecast by thermodynamic calculations on CALPHAD. It is possible to generate a very large number of compositions.
- After analyses of the simulations, some compositions are selected and achieved by fusion of powder. The microstructure is investigated.
- Following the results of the previous step, some compositions are chosen and coated samples are tested.

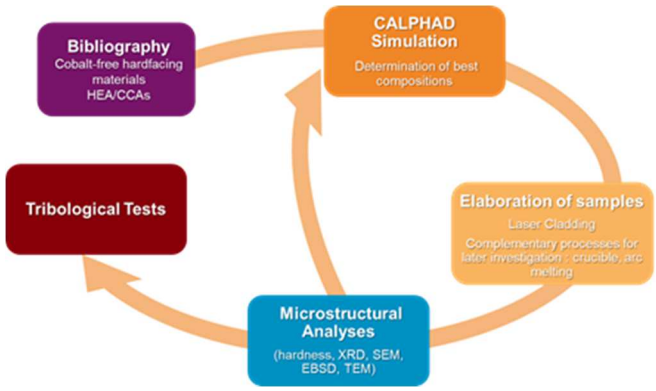

Fig. 1: Proposed methodology for exploring HEA/CCAs

Of course, multiple loops can be necessary to explore different compositions before to converge toward an optimal result. In the next sections, we show the work that has been initiated trying to follow this methodology.

2. Selection of alloys

2.1. Selection of a family of alloys

Considering the bibliography analysis and the targeted applications, considerations can be made to focus our selection of alloy family:

1. As the coating has to be made on stainless steel, it is desired that the chosen alloys should generate a good metallurgical bonding with the substrate. This is in favor of a reach (Fe,Cr,Ni)-rich composition.
2. No cobalt is allowed. Moreover, for the same reason than cobalt, niobium amount should be limited.
3. Hardfacing property implies that the material would have a good compromise between hardness and elasticity. Globally, hardness is usually above 400Hv. Consequently, the alloys should contain hard phases.
4. Good corrosion behavior would be considered. In our study, we consider wear test in Argon gas environment to facilitate the wear tests.

Combining these points, it can be proposed to retain a general formulation as $Fe_{x1}Ni_{x2}Cr_{x3}Mn_{x4}Mo_{x5}Ti_{x6}V_{x7}Zr_{x8}Nb_{x9}Al_{x10}$ with $[x1…x10] \geq 5at\%$.

As combinatorial metallurgy our manufacturing process consists in the fusion process of a mixture of powder, it has been decided to avoid using Mn, due to low boiling point compared to the other elements. Adding cost and powder quality constraints, it has be decided to consider the first alloy family $Fe_{x1}Ni_{x2}Cr_{x3}Mo_{x4}Ti_{x5}$. In this article, we present the results obtained for 3 alloys: $(FeNiCr)_{80}Mo_{10}Ti_{10}$, $(FeNiCr)_{80}Mo_{15}Ti_5$, and $(FeNiCr)_{90}Mo_5Ti_5$.

2.2. Thermodynamics simulations

Thermodynamic calculations using CALPHAD/Thermo-Calc® supported by TCHEA1 database were performed. As said in the introduction, CALPHAD calculation was performed to have an estimation of the phases present and their composition. In the family of alloy FeNiCrMoTi, Fig. 2 shows the solidification curves calculated by CALPHAD at thermodynamical equilibrium for two of the three alloys with the TCHEA1 database: $(FeNiCr)_{90}Mo5Ti_5$ and $(FeNiCr)_{80}Mo_{10}Ti_{10}$.

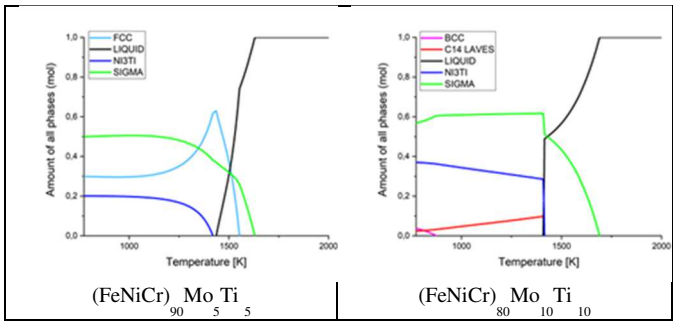

$(FeNiCr)_{90}Mo_5Ti_5$ $(FeNiCr)_{80}Mo_{10}Ti_{10}$

Fig. 2. CALPHAD simulation of solidification of two alloys

Calculations on the $Mo_{10}Ti_{10}$ and Mo_5Ti_{15} alloys predict the presence of four phases: sigma, BCC, Ni_3Ti and C14 Laves phase. BCC phase should be absent of $Mo_{10}Ti_{10}$ because of its low formation temperature, and C14 Laves phases is supposed to transformed into Ni_3Ti upon cooling. During the cooling of Mo_5Ti_{15}, C14 Laves phases and sigma phase are supposed to transform into Ni_3Ti and BCC phase, respectively. $Mo_{15}Ti_5$ is predicted to have a high sigma phase amount with FCC and Ni_3Ti phase. A small amount of BCC phase is also predicted at low temperature and should not be observed experimentally.

Table1 presents the CALPHAD calculation results with Gulliver-Scheil approximation (as LMD solidification is supposed to lead to an out-of-equilibrium solidification) at the end of solidification on the three alloys with the TCHEA1 database. This hypothesis increases the number of phases predicted in the alloys. FCC and C14 Laves are predicted in all alloys in addition to the equilibrium phase predicted. The only exception is the substitution of Ni_3Ti in by a $D0_{19}$ phase in the Mo_5Ti_5 alloy.

Table 1. CALPHAD calculations for the three alloys with Gulliver-Scheil approximation

Alloy	Phases predicted after cooling CALPHAD + Gulliver-Scheil approximation
$(FeNiCr)_{90}Mo_5Ti_5$	Sigma, FCC, $D0_{19}$, C14 Laves
$(FeNiCr)_{80}Mo_{10}Ti_{10}$	Sigma, FCC, BCC, Ni_3Ti, C14 Laves
$(FeNiCr)_{80}Mo_{15}Ti_5$	Sigma, FCC, Ni_3Ti, C14 Laves

These calculations evidence the possibility to obtain alloys composed of a mixture of medium hard matrix and hard phase, which hardness and fracture toughness has to be determined in the study. This can be related to the Tribaloy T700 microstructure. Now, we present the elaboration of the alloys by LMD and the results obtained.

3. Elaboration of alloys

3.1. Experimental setup

The manufacturing of samples has been achieved on an OPTOMEC machine with four powder feeders (Fig. 3). The laser used is an IPG 3kW CW (λ=1070nm), a core fiber of 400µm. A coaxial nozzle has been used.

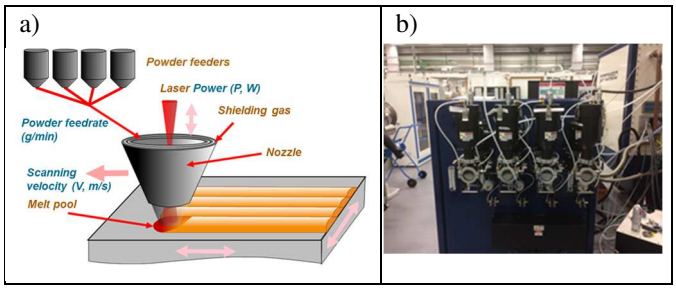

Fig. 3. LMD system: a) LMD principle b) the four powder feeders

It can be difficult to get a homogenous melting of the material from the mixture of powders [26]. Thus, the in situ fusion is better achieved with a relatively large melt pool and low speed. Therefore, the optical configuration has been chosen to provide a defocused laser beam spot size of about 2mm diameter.

3.2. Manufacturing of samples

Following the selection of compositions obtained from CALPHAD calculations, different samples have been prepared.

First, single elements have been provided in powder form: Ni, Fe, Cr, Mn, Mo, Ti, Al, Zr, Si. Moreover, it has been decided to provide a powder of ($Ni_{100/3}Fe_{100/3}Cr_{100/3}$) at% as a basis of our experimental investigation. This powder will be blended with others to generate the samples.

Two types of samples have been elaborated by laser cladding:

- wall structures with or without graded composition, typically of about 30mmx20mmx2mm (example in Fig. 4). They are used for combinatorial investigation purpose. The process parameters used were:
  - ✓ Power (P)=1800W (first layer), 1400W (following layers),
  - ✓ Travel speed (V)=250mm/min,
  - ✓ Powder flow rate (Dp)= 6g/min.

  There are mainly used to generate a rapid screening of a selected range of compositions.
- coatings: After a selection of some compositions from their microstructural analysis, some coatings have been achieved for wear tests. Coatings of about 40mmx40mm on about 4mm thickness are elaborated for the alloys to be tested in tribology (example in Fig. 5). The parameters (P,V,Dp) are the same as chosen for the wall structures. Hatching Distance (HD) between two tracks is 1.8mm. The coatings consist in 5 layers of about 0.8mm each.

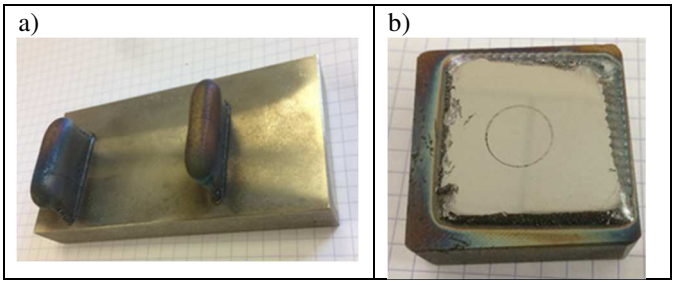

Fig. 4. Example of samples elaborated by laser cladding: a) wall structure with graded composition, b) Laser cladded coatings for wear tests

Two coatings of each composition $(FeNiCr)_{90}Mo_5Ti_5$, $(FeNiCr)_{80}Mo_{10}Ti_{10}$ and $(FeNiCr)_{80}Mo_{15}Ti_5$ have been elaborated for the microstructure analysis and the wear tests.

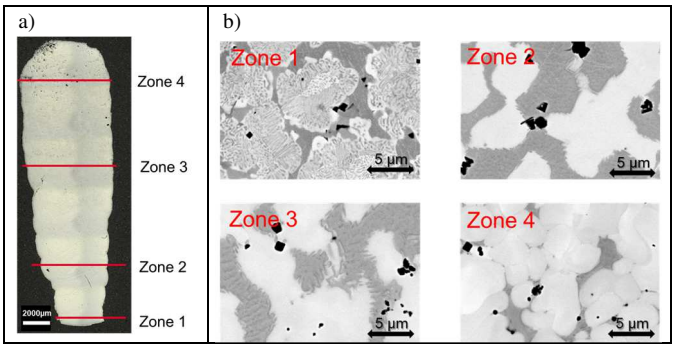

Fig. 5. Example of graded wall in NiFeCr+Mo+Ti : a) Vertical cut macrograph, b) cross-section micrographs in defined zones (BSE)

The composition of each zone of the wall structure is presented in Table 2. It can be seen that the measured composition globally follows the programmed one. The small deviations are most probably due to thedilution of the substrate.

Table 2. Programmed and measured (EDX) composition of the zones of the wall presented in Fig.5.

Zone	Programmed content (%at)			Measured content (%at)		
	$Ni_{100/3}Fe_{100/3}Cr_{100/3}$	Mo	Ti	$(Ni,Fe,Cr)_{total}$	Mo	Ti
1	85	10	5	88,9	7.3	3.8
2	83	12	5	85.6	10.3	4.1
3	81	14	5	81.0	13.4	5.6
4	79	16	5	77.1	16.2	6.7

The elaborated samples have been analyzed by SEM/SE+BSE, XRD and EBSD and the results compared to the thermodynamically simulations. The results are presented in the next sections.

3.3. $(FeNiCr)_{90}Mo_5Ti_5$ sample

The alloy is mainly composed of a FCC matrix containing a medium amount of sigma phase presented in Fig. 6. A small presence of Ni_3Ti and titanium nitride have been detected. Although this is close to TCHEA1 CALPHAD calculation at equilibrium solidification, the proportion of phases slightly differs and TiN has not been predicted. Out of equilibrium calculation does not give more correlated results.

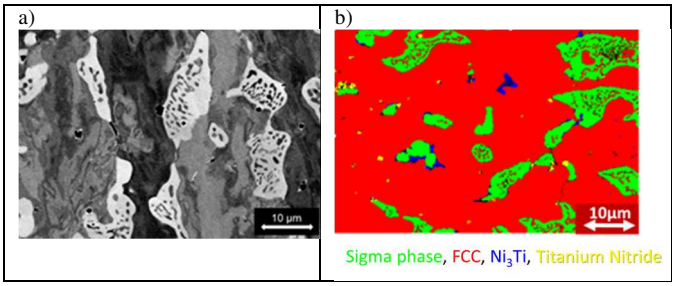

Fig. 6. a) SEM/BSE image and b) EBSD phase determination. of $(FeNiCr)_{90}Mo_5Ti_5$ sample

Globally, the sample exhibits a microhardness of about 550 HV_{10} (5.40 GPa).

3.4. $(FeNiCr)_{80}Mo_{10}Ti_{10}$ sample

The microstructure of this alloy is presented in Fig.7. Due to the high content of Mo, the alloy is mainly composed of a sigma phase surrounded by C14 Laves p.hases and additional Chi phase, Ni3Ti and TiN in small amount.

This differs significantly from TCHEA1 CALPHAD calculation at equilibrium solidification. Particularly, no BBC phase has been found in the sample. Out of equilibrium calculation does not give more correlated results.

Globally, the sample exhibits a microhardness of about 755 HV_{10} (7.40 GPa). The high content of sigma phase has a clear impact on the increase of hardness compared to $(FeNiCr)_{90}Mo_5Ti_5$ sample.

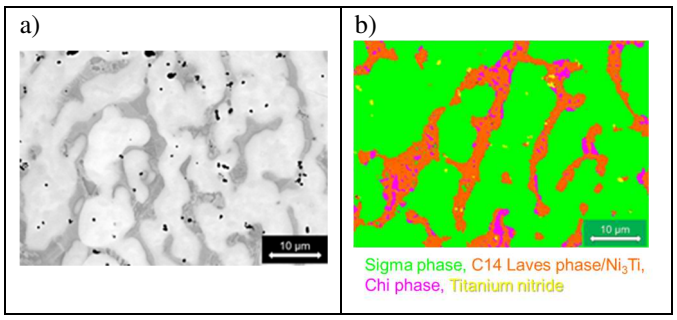

Fig. 7. a) SEM/BSE image and b) EBSD phase determination of $(FeNiCr)_{80}Mo_{10}Ti_{10}$ sample

3.5. $(FeNiCr)_{80}Mo_{15}Ti_5$ sample

The microstructure of this alloy is presented in Fig. 8.

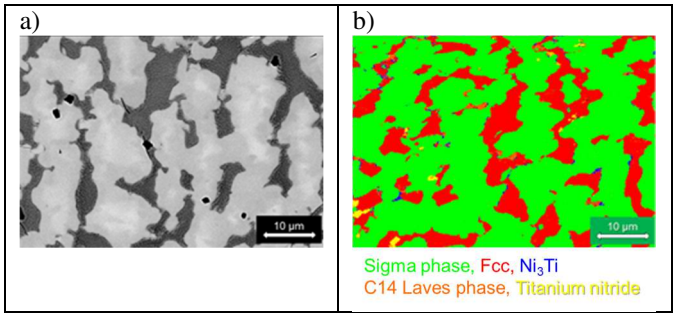

Fig. 8. a) SEM/BSE image and b) EBSD phase determination of $(FeNiCr)_{85}Mo_{10}Ti_5$ sample

As for $(FeNiCr)_{80}Mo_{15}Ti_5$, the high content of Mo has induced the solidification of the sigma phase as the main phase surrounded by FCC and additional C14 Laves, Ni3Ti and TiN phases in a very small amount. For this composition, except for TiN, the out of equilibrium calculations globally fits with the experimental results.

Globally, the sample exhibits a microhardness of about 700 HV_{10} (6.9 GPa). This is comparable to the $(FeNiCr)_{80}Mo_{10}Ti_{10}$ sample.

Globally, the alloys exhibit a fine a relatively equiaxed microstructure composed, as expected, by a high content of hard phases. It is now necessary to make the wear tests for comparing their tribological behaviors.

4. Tribology tests

4.1. Experimental setup

Pin-on-disk tests were performed on a rotary pin-on-disk tribometer THT from CSM Instrument. In accordance with regular tests previously defined [11,12], tests were performed with a ruby ball of 6mm diameter, a Hertz pressure of 1GPa, rotation speed of 5mm/s for a total distance of 100m under argon atmosphere with constant argon flushing and room temperature. The load and the sliding speed are representative of the conditions that would be encountered in targeted applications. The ruby ball is not worn out during the tests and it does not participate to the formation of a third body, allowing an easiest comparison between different alloys. The goal of the tribological analysis is to compare the wear behavior of the CCAs with the Stellite reference.

Samples were first surfaced and then gradually polished to finish with a 2400 grade SiC paper. Friction coefficient was measured with two force sensors to minimize errors coming from the temperature changes. Wear rate was estimated by measuring the lost volume with an interferometric microscope.

4.2. Tribology tests

Four samples $(FeNiCr)_{90}Mo_5Ti_5$, $(FeNiCr)_{90}Mo_{10}Ti_{10}$, $(FeNiCr)_{90}Mo_{15}Ti_5$, and Stellite 6 as the reference material have been prepared by laser cladding. The friction coefficients are measured along the wear test and wear rates after 100m driving distance (see Fig. 9 for results).

Globally, the CCAs exhibit similar wear properties. Their friction coefficients stabilize at about 0.4, which remains higher than Stellite 6 (close to 0.2). However, the wear rate of the three tested CCAs remains lower that of Stellite 6.

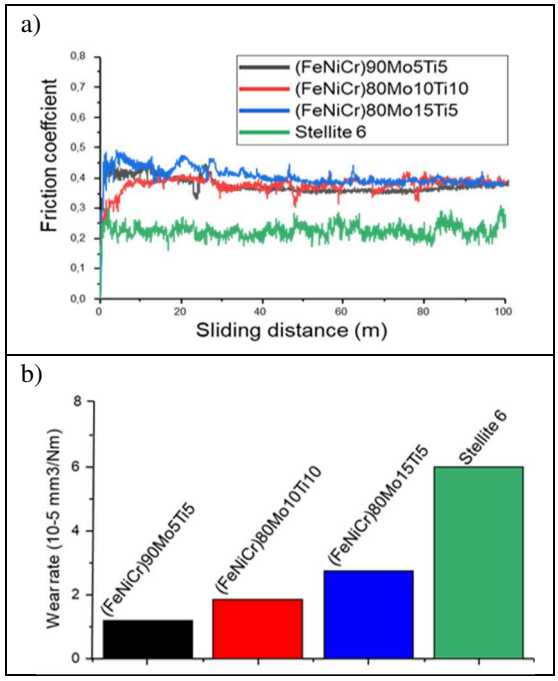

Fig. 9. a) Friction coefficient along wear, and b) wear rate for the 3 alloys

4.3. Discussion

First, the three alloys exhibit a similar abrasive wear. Although a very good argon gas protection, an oxide film is formed by the heat induced by dissipated energy in the contact decreasing the friction coefficient and protecting the alloys by reducing the contact surface between the ball and the coating.

This film is subjected successively to growth, abrasion, formation of cracks and partial delamination. This delamination process results in a significant variation in the friction coefficient. Depending on the alloy, certain variations are visible on the size of the particles generated by the damage to the surface. These oxide particles can contribute to abrasion: the smaller the particles, the more they can be trapped inside the contact and contribute to the abrasion of the surface. The phase composition can clearly lead to different wear behaviors.

So far, it is unclear whether the surface of the samples is damaged differently depending on their composition. In addition, wear tests are planned to assess the repeatability of the measurements.

5. Conclusion and perspectives

In this article, we have proposed a new approach for the elaboration of cobalt free hardfacing coatings. From the bibliography, we have shown that new approaches in metallurgy and material processing is a good opportunity for this purpose. LMD is a very versatile tool for a combinatorial metallurgy approach that can be used for the exploration of the new family alloys of HEA/CCAs material. Moreover, we have proposed an iterative methodology that combines simulations with CALPHAD calculations and combinatorial elaboration of materials by the in-situ laser fusion of powders. This study has recently started and an example bas been presented on three alloys.

It is clear that each step has some drawbacks as prediction errors due to incomplete thermodynamic database, uncertainty in melting of powders (impurities, segregation of powders, melting point issue,…). Although this has to be improved, promising results have been obtained for the wear behavior of the proposed CCAs. If their friction coefficients are still higher than Stellite 6, they would be acceptable for a large range of applications. Moreover, the three alloys exhibit a smaller wear rate compared to Stellite 6 and their wear mechanism in mainly abrasive mode are promising characteristics for galling conditions.

The study will be extended on other type of alloys from the initial group, improving simulation and experimental tools for their development.

References

[1] D.H.E. Persson, S. Jacobson, S. Hogmark, Effect of temperature on friction and galling of laser processed Norem 02 and Stellite 21, Wear 255, 2003, pp.498–503

[2] D. H. E. Persson, Laser processed low friction surfaces, Dissertation for the degree of Licentiate of Philosophy in Materials, Materials Science Division, the Ångström Laboratory, Uppsala University, Sweden, March 2003

[3] C. B. Bahn, B. C. Han, J. S. Bum, I. S. Hwang, Chan Bock Lee, Wear performance and activity reduction effect of Co free valves, in PWR environment, Nuclear Engineering and Design 231, 2004, pp. 51–65

[4] M. Corchia, P. Delogu,, F. Nenci,. Microstructural Aspects of Wear-Resistant Stellite and Colmonoy Coatings by Laser Processing, Wear, Volume 119, 1987, pp. 137-152

[5] Kashani, A. Amadeh, & H. Ghasemi, Room and high temperature wear behaviors of nickel and cobalt base weld overlay coatings on hot forging dies. Wear, 262(7-8), 2007, pp. 800-806,

[6] Qian Ming, L.C. Lim, Z.D. Chen, Laser cladding of nickel-based hardfacing alloys, Surface and Coatings Technology 106, 1998, pp. 174-182

[7] D. Kesavan, & M. Kamaraj, The Microstructure and High Temperature Wear Performance of a Nickel Base Hardfaced Coating, Surface and Coatings Technology, 204(24), 2010, pp. 4034-4043

[8] V.D. Tran, P. Aubry, C. Blanc, J. Varlet, T. Malot, Laser Cladding And Tribocorrosion Testing Of Cobalt-Free Hardfacing Coatings For Fast Neutron Reactor, Proc. of ICALEO 2014, 2014, paper #203

[9] C. Navas, R. Colaço, J. Damborenea, & R. Vilar, Abrasive Wear Behavior of Laser Clad and Flame Sprayed-Melted NiCrBSi Coatings, Surface and Coatings Technology, 200(24), 2006, pp. 6854-6862

[10] K. Komvopoulos, K. Nagarathnam, Processing and Characterization of Laser-Cladded Coating Materals, J. of Engineering Materials and Technology, vol. 112, (1990), pp. 131-143

[11]P.Aubry, C.Blanc, I.Demirci, M.Dal, T.Malot, H. Maskrot, Laser Cladding of Nickel Base Hardfacing Materials: Influence of Process Parameters, Proc. of ICALEO 2016 (2016), San Diego, Paper #303

[12] P. Aubry, C. Blanc, I. Demirci, M. Dal, T. Malot, and H. Maskrot, Laser cladding and wear testing of nickel base hardfacing materials: Influence of process parameters, J. Laser Appl. 29, 022504 , 2017, pp. 1-9

[13] P.Aubry, C.Blanc, I.Demirci, M.Dal, T.Malot, Analysis of nickel based hardfacing materials manufactured by laser cladding for Sodium Fast Reactor, Proc. 9th Int. Conf. Photonics Tech. LANE 2016, Physics Procedia, (2016), Procedia CIRP Volume 74, 2018, pp. 210-213

[14] B. Cantor, I. T. H. Chang, P. Knight, and A. J. B. Vincent, "Microstructural development in equiatomic multicomponent alloys," Mater. Sci. Eng. A, vol. 375–377, no. Supplement C, pp. 213–218, Jul. 2004,

[15] J.-W. Yeh et al., "Nanostructured High-Entropy Alloys with Multiple Principal Elements: Novel Alloy Design Concepts and Outcomes," Adv. Eng. Mater., vol. 6, no. 5, pp. 299–303, May 2004,

[16] Y. H. Jo et al., "Utilization of brittle σ phase for strengthening and strain hardening in ductile VCrFeNi high-entropy alloy," Mater. Sci. Eng. A, vol. 743, pp. 665–674, Jan. 2019

[17] H. Abed, F. Malek Ghaini, and H. R. Shahverdi, "Characterization of Fe49Cr18Mo7B16C4Nb6 high-entropy hardfacing layers produced by gas tungsten arc welding (GTAW) process," Surf. Coat. Technol., vol. 352, pp. 360–369, Oct. 2018

[18] J. Zeisig et al., "Microstructure and abrasive wear behavior of a novel FeCrMoVC laser cladding alloy for high-performance tool steels," Wear, vol. 382–383, pp. 107–112, Jul. 2017

[19] N. Ley, S. S. Joshi, B. Zhang, Y.-H. Ho, N. B. Dahotre, and M. L. Young, "Laser coating of a CrMoTaWZr complex concentrated alloy onto a H13 tool steel die head," Surf. Coat. Technol., Feb. 2018,

[20]H. Dobbelstein, M. Thiele, E. L. Gurevich, E. P. George, and A. Ostendorf, "Direct Metal Deposition of Refractory High Entropy Alloy MoNbTaW," Phys. Procedia, vol. 83, no. Supplement C, pp. 624–633, Jan. 2016

[21] H. Dobbelstein, E. L. Gurevich, E. P. George, A. Ostendorf, and G. Laplanche, "Laser metal deposition of a refractory TiZrNbHfTa high-entropy alloy," Addit. Manuf., vol. 24, pp. 386–390, Dec. 2018

[22] H. Dobbelstein, E. L. Gurevich, E. P. George, A. Ostendorf, and G. Laplanche, "Laser metal deposition of compositionally graded TiZrNbTa refractory high-entropy alloys using elemental powder blends," Addit. Manuf., vol. 25, pp. 252–262, Jan. 2019

[23] The Calphad Maetodology, https://www.thermocalc.com/products-services/databases/the-calphad-methodology/

[24]G. Bracq, M. Laurent-Brocq, L. Perrière, R. Pirès, J.-M. Joubert, and I. Guillot, "The fcc solid solution stability in the Co-Cr-Fe-Mn-Ni multi-component system," Acta Mater., vol. 128, pp. 327–336, Apr. 2017

[25] D. B. Miracle, J. D. Miller, O. N. Senkov, C. Woodward, M. D. Uchic, and J. Tiley, "Exploration and Development of High Entropy Alloys for Structural Applications," Entropy, vol. 16, no. 1, pp. 494–525

[26] Dobbelstein H., Thiele M., Evgeny L.GurevichaEaso P. George E.P., Ostendorf, Direct Metal Deposition of Refractory High Entropy Alloy MoNbTaW, Physics Procedia, Vol. 83, 2016, pp. 624-633